Shear Rheology of Asymmetric Star Polymers

Amy K. Tezel and L. Gary Leal*

Department of Chemical Engineering, University of California at Santa Barbara, Santa Barbara, California 93106

Received January 22, 2006; Revised Manuscript Received April 14, 2006

ABSTRACT: Asymmetric stars provide a challenging test of the tube model, which has been successfully applied to both linear chains and symmetric star polymers. Previous work has shown that the tube model can be applied with some success to asymmetric stars in the linear viscoelastic regime. This work considers asymmetric polybutadiene stars in the nonlinear regime, where the shear flow plays a significant role in the response of the asymmetric star. In the nonlinear regime it is expected that convective constraint release will be the dominant relaxation mechanism for the asymmetric star polymers, as has been demonstrated for linear and symmetric star polymers. By using two-color flow birefringence, the shear stress and first normal stress difference as a function of shear rate for entangled asymmetric stars can be determined. The experimental results are then compared with a tube-based model that includes convective constraint release and are found to be in reasonable agreement.

1. Introduction

The majority of fundamentally oriented studies of the rheology of entangled polymers has focused on either linear chains or symmetric stars, where each arm has the same number of entanglements and the same molecular weight.[1−10] The linear viscoelastic properties of linear chains and symmetric stars are well described and understood under the ansatz of the tube model,[11−14] and models have also been proposed for the nonlinear properties of these systems.

Asymmetric stars provide a further test of the tube model and our current understanding of how entangled polymers relax. Beginning with a linear chain, which is well understood in the linear viscoelastic regime,[15] the question is how the dynamics change if a short arm is placed in the middle of the linear chain? The follow-up question is, how do the effects of this short arm change as its molecular weight is increased until it is finally equal to half the molecular weight of the linear chain, at which point there is a symmetric three-arm star? This was precisely the framework used in an important paper by Frischknecht and colleagues, who compared linear viscoelastic data with predictions based on the most straightforward adaptation of the tube model. The details of this work and of follow-up studies will be discussed shortly.[16]

The primary purpose of the present investigation is to consider the shear rheology of asymmetric stars in the *nonlinear* regime, which has not been previously studied. It is expected, on the basis of previous studies for both linear polymers and symmetric star solutions, that the relaxation mechanism that is known as convective constraint release (CCR) will be dominant once the shear rate exceeds the inverse of the longest linear relaxation time. CCR describes the release of entanglement constraints as a chain end moves away from the neighborhood of a nearby chain due to relative "convective" motions of the chains. The dominant contribution to CCR normally comes from the continual retraction of the chains from the extra contour length that is generated by affine deformation with the flow.[17] The rate of relaxation by this process increases in proportion with the shear rate. Our recent studies[4,18] of symmetric stars demonstrated that CCR-based relaxation of the arms could be described via the exact same theoretical model of CCR that had previously been developed for linear chains, including even the numerical prefactors. An obvious question is whether this same result can also be used for asymmetric stars, which can be viewed as initially relaxing like a star, followed by relaxation as a linear chain once the short arm is completely relaxed.

In the present paper, a series of four polymers, including a "2-arm" star (linear chain), two asymmetric stars, and a 3-arm symmetric star, have been studied in shear flow using rheooptic techniques, for Weissenberg numbers of order one. A nonlinear model, similar to that presented in our recent work on symmetric stars and incorporating the same model for CCR, will be discussed and compared to the experimental results.

2. Single Batch Synthesis of a Series of Asymmetric Polybutadiene Stars

To facilitate a study of the similarities and differences in behavior between linear polymers, asymmetric stars, and symmetric stars, the ideal system is a series of polymers having an identical backbone, but with a third arm of varying length located at the center of the backbone. Many of the previous studies of the linear rheology of asymmetric stars have been limited by having polymers with very similar, but not identical, backbones, thus limiting direct comparisons. The difficulty of producing such a series of polymers is the need to produce a very large batch of backbone chains.

The general synthesis procedure for an asymmetric star is described in the literature.[19,20] The present study considers butadiene polymerized anionically to make polybutadiene. However, the process is similar for a variety of monomers. First, the short arm is synthesized using anionic polymerization. The arm is then reacted with $MeSiCl_3$, where the chlorosilane linking agent is added in huge excess. This is done to ensure that each chlorosilane molecule that reacts will react with only one linear chain. The majority of the chlorosilane is unreacted and so is removed from the reaction flask by vacuum distillation. Simultaneously, a large batch of long arms must be synthesized anionically. This batch of arms is to be used for the linear chain, the symmetric star, and the backbone of each of the asymmetric stars. The long arms are then added in excess to the chlorosilane that has one short arm attached and allowed to react to produce the asymmetric stars. The synthesis of the linear chain involves

* Corresponding author. E-mail: lgl20@engr.ucsb.edu.

10.1021/ma0601520 CCC: $33.50 © 2006 American Chemical Society
Published on Web 05/23/2006

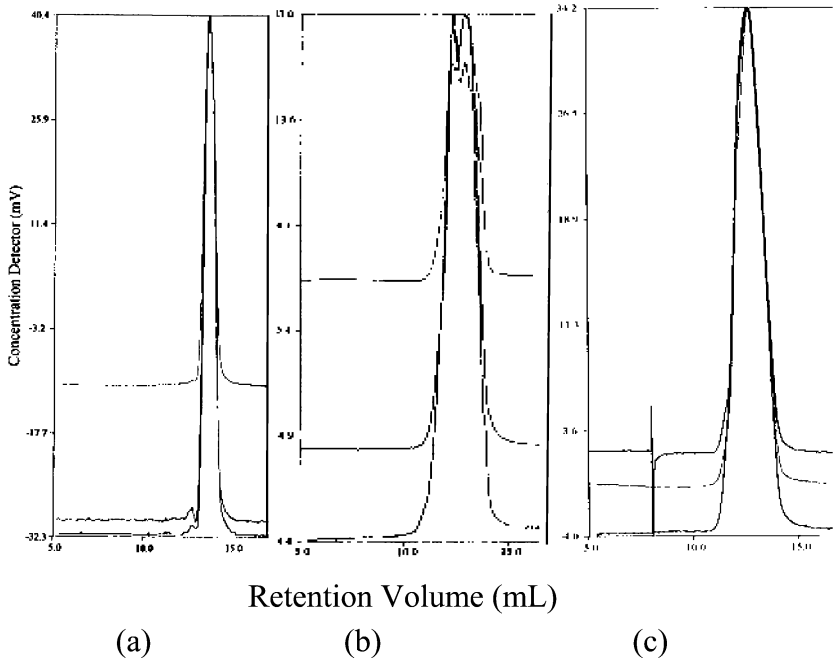

Figure 1. Chromatogram shapes for star B during the different stages of synthesis: (a) the monodisperse short arm; (b) the unpurified asymmetric star; (c) the final purified asymmetric star B.

Table 1. Molecular Weights and Polydispersity Indices for Stars A−D, Including Details about the Third (Short) Arm

		third arm		total polymer		
polymer	description	M_n	PDI	M_n, theoretical	M_n, actual	PDI
star A	symmetric	69 200	1	208 000	206 000	1.014
star B	AS-longest	49 400	1.007	188 000	179 000	1.045
star C	AS-shortest	27 600	1	166 000	162 000	1.078
D	linear	0	NA	138 000	140 000	1.044

transferring some of the long arms to a clean flask and then adding a dichlorosilane linking agent, while the synthesis of the three-arm star requires the addition of a trichlorosilane linking agent.

In practice, the most difficult parts of the synthetic procedure are threefold. First, to make enough of each polymer sample, it is necessary to produce a large amount of the backbone arms. While typical anionic synthesis yields up to 5 g of polymer, this particular synthesis required close to 50 g. Second, the backbone arms have to be transferred to the reaction flasks that contain the short arms. But the transfer has to be carried out without allowing the addition of any water or air to the system. Typically such a transfer would be done using a chenula or small metal tube that uses nitrogen gas to push the polymer solution from one flask to the other. Our solution of long arms, however, was too viscous to allow for such a transfer. Instead, a piece of glassware was made to allow for a gravity driven transfer, which could be completed without killing any of the living polymer chains (as would happen if water entered the system, even in small amounts). Third, the final reaction linking the two long arms to the active chlorosilane must be done with excess linear chain to ensure that the resulting polymer is in fact a three-arm star. This leads to the necessity of purifying the final product to separate out the unreacted linear chains from the stars. This purification by fractional precipitation becomes increasingly difficult as the molecular weight difference between the two fractions is decreased. An optimization of this purification must be made to obtain the lowest polydispersity final product of the desired molecular weight, while maintaining an adequate amount of sample with which to perform the desired experiments. This requires numerous repetitions of the fractional separation.

The molecular weights and polydispersity indices of the polybutadiene precursor arms and the final polybutadiene stars are given in Table 1. The asymmetric polybutadiene stars had a microstructure of 9% 1,2 addition and 91% 1,4 addition, with half of that being of the cis conformation and the other half being of the trans conformation. Figure 1 shows the chromatograms from the short arm, the unpurified asymmetric star, and the final purified asymmetric star, all for star B.

Our primary objective was to examine the response of this series of polymers A−D to steady shear using the two-color flow birefringence apparatus, described previously by Tezel et al.[4] To perform these experiments using the Couette shear cell, a sample size of ∼5 g is needed. The amount of the purified stars was less than 1 g in each case. Therefore, the stars were put into solution in a low molecular weight polybutadiene at 12.5 wt %. The solvent had the trade name Ricon 157 from Sartomer Co. Its microstructure was 70% vinyl (1,2 addition) and had a number-average molecular weight of 1800 g/mol. In addition to allowing for a large enough sample size with which to perform the experiments, the use of a viscous solvent, as opposed to a less viscous solvent, slowed down the polymer dynamics, allowing easier experimental access to relevant time scales.

3. Linear Viscoelasticity

Recent work for both linear polymers and symmetric stars has led to linear viscoelastic predictions via the tube model framework for the storage and loss moduli as functions of frequency that match quantitatively with experimental results.[12,15] If the tube model can successfully describe linear and symmetric star polymers, then one would expect that the same framework and relaxation mechanisms should be capable of

being extended to describe asymmetric stars. A significant test of this hypothesis was published by Frischknecht et al. in 2002, with the apparent result that the diffusion of the branch point and reptation of the remaining chain after the short arm has relaxed did not occur as expected. It was anticipated by Frischknecht et al. that after each complete retraction of the short arm the branch point should be able to hop a distance related to the tube diameter. In this framework, the diffusion constant of the branch point, D_b, can be described via the following equation:

$$D_b = \frac{(pa_h)^2}{2\tau_s^*} \tag{1}$$

where a_h is the diameter of the tube, τ_s^* is the relaxation time scale for the short arm, and p is a dimensionless parameter of order one that describes the mean hopping distance of the branch point. Current understanding of the tube model would suggest that a_h should correspond to the diameter of the dilated tube, a_d. However, Frischknecht and colleagues found that their experimental data for G' and G'' for a series of asymmetric stars were best fit by assuming that $a_h = a$, namely the undilated tube diameter. The best-fit value for p was found to become smaller as the short arm gets shorter. Physically, the latter result would suggest that reptation is increasingly inhibited by the drag of the relaxed short arm as its molecular weight is decreased. Clearly, this does not make intuitive sense, as was recognized by the authors. The apparent lack of tube dilation is also a puzzle.

Because branch point motion is also important for more highly branched architectures such as pom-poms and combs, the value of p has been studied by other investigators for other types of polymers.[21] Some investigators assume that p must be constant, with common choices being $p = \sqrt{1/12}$ or $p = \sqrt{1/6}$, based on best fits with experimental data.[21,22] Other recent studies have proposed that p depends on the length of the short arm[23] or, similarly, on the fraction of the long arms that remain unrelaxed at the time that the short arm is completely relaxed.[16] In particular, the recent work of Lee, Fetters, and Archer provides a convincing case for the result[16]

$$p^2 = (2Z_{AR})^{-1} \tag{2}$$

where Z_{AR} is the number of unrelaxed entanglements in each of the long arms at the time of complete retraction of the short arm. Using this model, p increases as the length of the short arm increases for asymmetric stars (assuming constant length for the long arms). The full model using this theoretical value of p was compared with the same experimental data used originally in the Frischknecht paper, with significantly improved agreement.

The question of whether the final relaxation by reptation occurs in a dilated or undilated tube still remains open. However, experimental evidence for asymmetric stars gives better agreement with predictions for an undilated tube unless the number of entanglements is extremely large when the dilated tube assumption does a better job.

Measurements of the storage and loss moduli (G' and G'', respectively) for all four solutions listed in Table 1 were taken over a range of temperatures by Michalis Kapnistos at the FORTH Institute (Crete). [Our measurements at UCSB were limited by lack of direct access to a rheometer with a wide range of accessible temperatures (especially low temperature reaching −50 °C).] Using time−temperature superposition, a master curve was created, showing G' and G'' over a wide range of frequencies using a reference temperature of 22 °C. These curves are given in Figures 2−5 for the four different solutions.

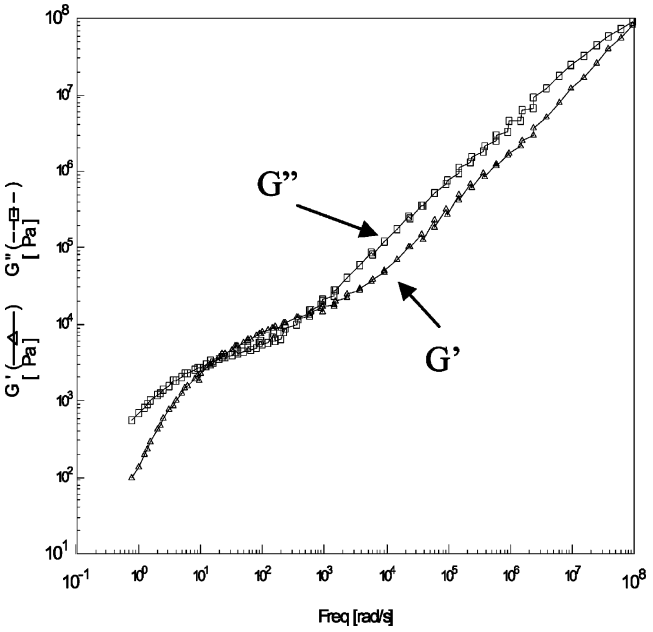

Figure 2. Storage (G') and loss moduli (G'') as functions of frequency for star A. Star A is a symmetric three-arm star solution with each arm having 4.7 entanglements.

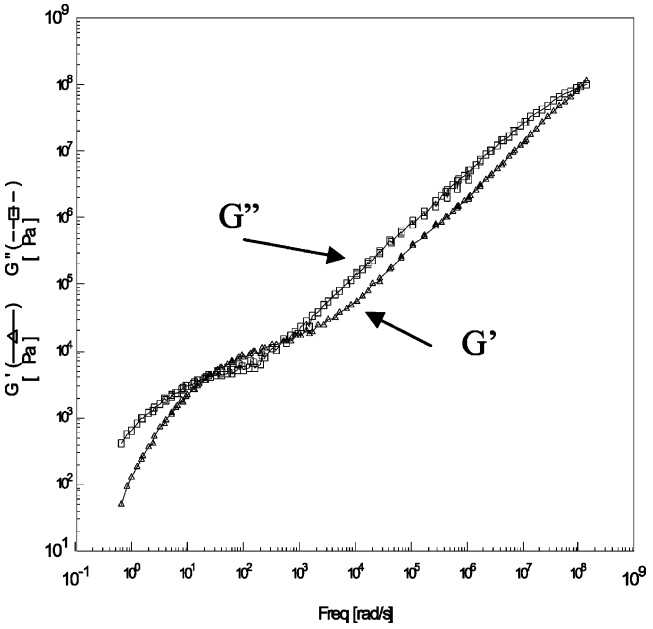

Figure 3. Storage (G') and loss (G'') moduli as functions of frequency for star B. Star B is an asymmetric three-arm star solution, with two long arms, each having 4.7 entanglements, and a short arm with 3.3 entanglements.

In the linear viscoelastic regime, the addition of a third arm is expected to have four important consequences:[16] (1) the peak in G'' should broaden with increasing length of the third arm, (2) the magnitude of the peak in G'' should decrease with increasing arm length, (3) the relaxation spectrum should broaden, and (4) the frequency of the G', G'' crossover should decrease with increasing arm length. All of these changes in the relaxation spectrum are the result of the branch point increasingly retarding the molecular relaxation, as the third arm increases in length. In the experimental data presented in Figures 2−5, the third and fourth predicted consequences are ob-

CDV

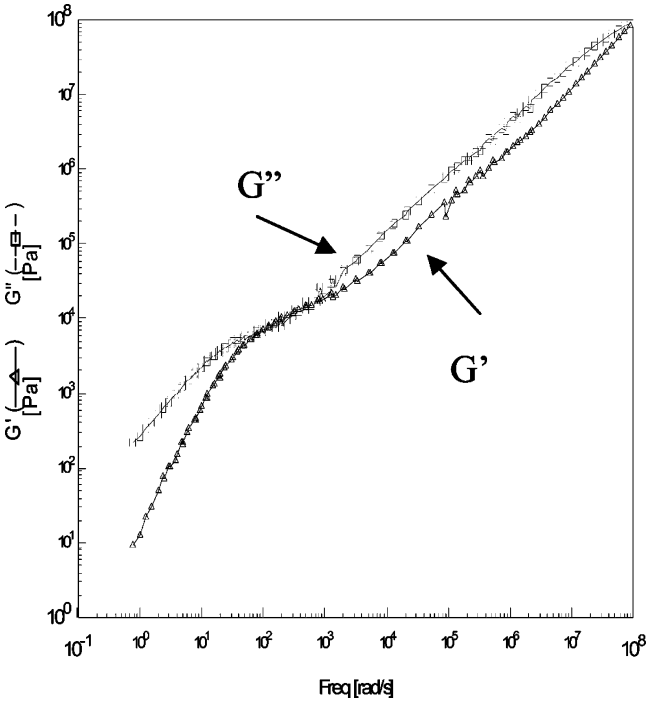

Figure 4. Storage (G') and loss (G'') moduli as a function of frequency for star C. Star C is an asymmetric three-arm star solution, with two long arms, each having 4.7 entanglements, and a short arm with 1.9 entanglements.

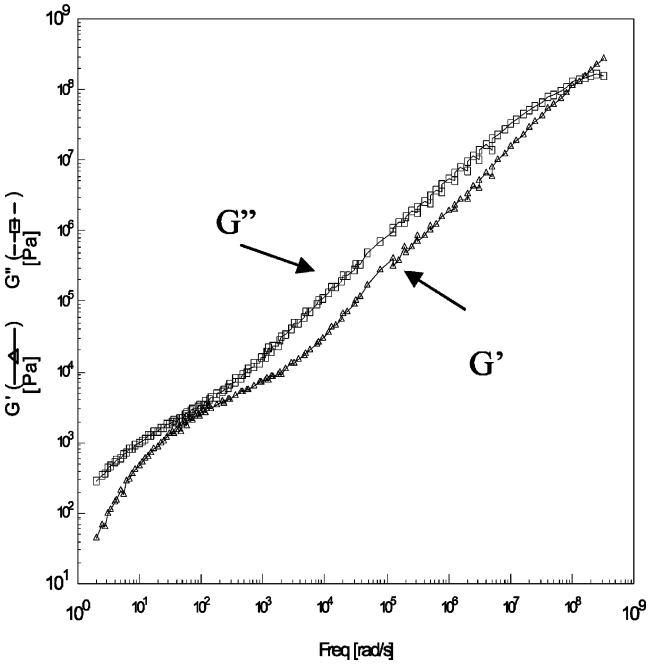

Figure 5. Storage (G') and loss (G'') moduli as a function of frequency for the linear polymer D, which has 9.4 entanglements per chain.

served: the width of the relaxation spectrum is increased as the length of the third arm is increased, and there is a monotonic decrease of the crossover frequency with increasing arm length. The first two features were not observed, however, because there is no obvious peak in G'' for any of the experimental data. Quite possibly this is due to the fact that the polymers being studied are in solution, as opposed to being studied in the melt. It has been suggested that the spreading out of the peak in G'' in solutions is due to local concentration fluctuations,[18] although this is still a topic of debate. Widening of the peak in G'' can also occur due to polydispersity. However, the polydispersity

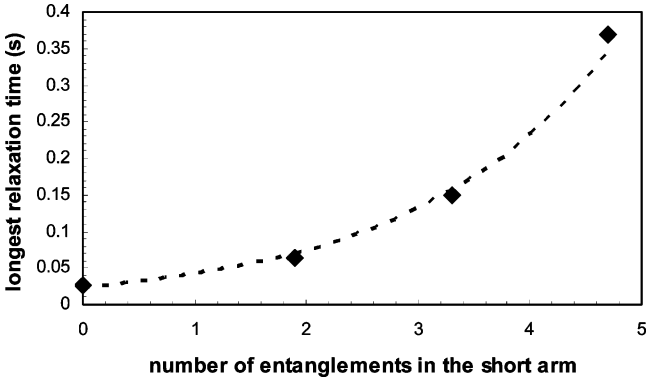

Figure 6. The longest relaxation time of each of the four polymers, plotted as a function of the number of entanglements in the short arm. The solid line shows an exponential data fit.

index of the polymers studied here is at most 1.078, and polydispersity alone cannot explain the lack of a G'' peak.

Comparisons between the measured relaxation moduli and model predictions based upon the linear viscoelastic model presented by Lee et al.[16] were made for the two asymmetric stars (stars B and C), as shown in Figures 7 and 8. The intrinsic Rouse relaxation time τ_e was used as a single fitting parameter, chosen based on obtaining a best fit in the terminal regime (the low-frequency crossover of G' and G''). The other parameters were fixed based upon literature values. In particular, the number of entanglements for each arm, Z_a, was calculated according to the formula

$$Z_a = \frac{M_a}{M_e}\phi^{\alpha} \tag{3}$$

with M_a being the molecular weight of the arm, as found in Table 1, and M_e being the literature value of 1850 for the entanglement molecular weight of polybutadiene melt.[24] The weight percent concentration of the polymer is denoted as ϕ, here having the value of 0.125, and α is the dilution parameter, which has been given a value of 1 based on a recent study for a series of solutions of symmetric polybutadiene stars.[18] G_N^0 is found by taking the literature value for a polybutadiene melt of 1.25 MPa[24] and multiplying by the concentration to the 2α power, again using a dilution parameter $\alpha = 1$. The values of the fixed parameters used in fitting the model to the experimental data are shown in Table 2. Also shown are the values of the empirically determined relaxation times, τ_e, as well as results for longest relaxation times. Figure 6 shows the dependence of the longest relaxation time upon the length of the third arm. The data can be fit using an exponential curve.

Examining Figure 7 for star B and Figure 8 for star C, we see that the quality of the fit between the experimental results and the model predictions, with the parameters estimated as described above, is reasonable at low frequencies but shows larger deviation at higher frequencies as the model underpredicts the magnitude of the response. The two main previous studies had already indicated that the current LV model for asymmetric stars does not yield quantitatively accurate predictions, even for polymer melts.[16] The main differences observed were a much less well-defined peak in G'' after the G', G'' crossover and an underprediction of the response at frequencies higher than the crossover frequency. To address these deficiencies in the fit between experiment and model, the approach of previous investigators was to use all of M_e, G_N^0, and τ_e as adjustable parameters, instead of just τ_e as in the present study. When this is done, there is much better agreement with the data, although

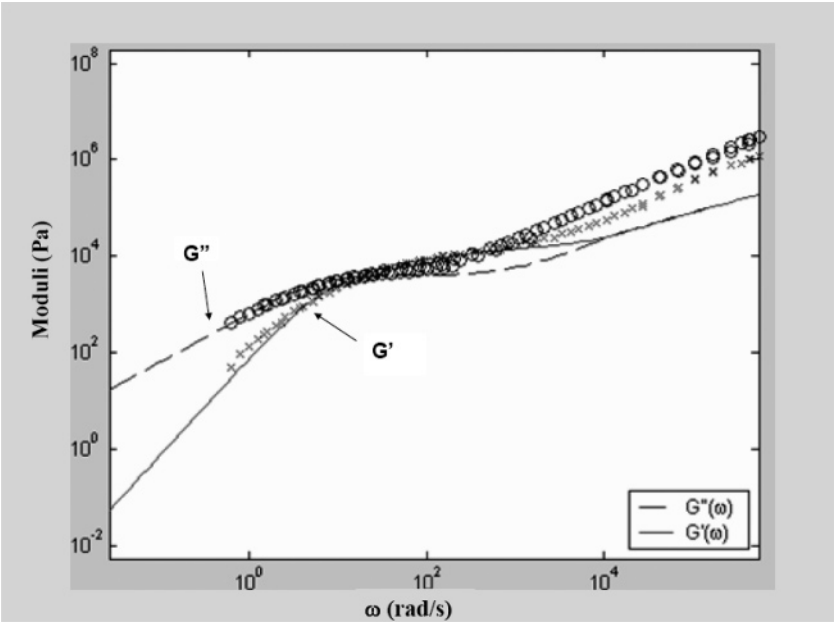

Figure 7. Comparison of experimental results and the predicted moduli for star B. The model predictions are based on the series of equations found in the appendix of Lee et al.[16]

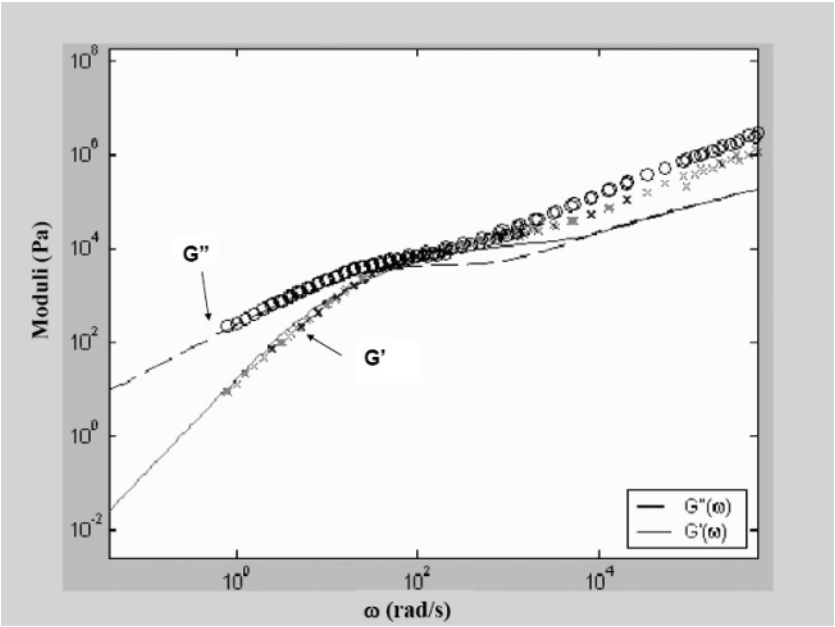

Figure 8. Comparison of experimental results and the predicted moduli for star C. The model predictions are based on the series of equations found in the appendix of Lee et al.[16]

Table 2. Parameters Used To Describe Stars A, B, and C and Linear Polymer D

	star A (symmetric)	star B	star C	linear D
Z_{long}	4.7	4.7	4.7	4.7
Z_{short}	0	3.3	1.9	4.7
G_N^0 (Pa)	19500	19400	19500	19500
p	NA	0.57	0.41	NA
τ_e (s)	3.5×10^{-5}	1.8×10^{-4}	8.3×10^{-5}	3.5×10^{-5}
$\tau_{longest}$ (s)	0.37	0.15	0.063	0.026

no single set of parameters is able to correctly capture both the high-frequency response and the low-frequency G', G'' crossover.

The comparisons in Figures 7 and 8 also show less dramatic behavior of G'' beyond the crossover frequency and an underprediction of the magnitude of the response at high frequencies. Here, τ_e was used as *the* sole adjustable parameter, with the aim of fitting the G', G'' crossover rather than the high-frequency data. So far as we are aware, this is the first application of the LV model for asymmetric stars in a solution rather than as melts, and this must be considered when looking for sources of deviation between the data and the model. The p value calculated by adjusting τ_e and finding the best fit of the model for star B is 0.57 and for star C is 0.41. This means physically that the branch point's ability to hop is hindered by increase in the MW of the short arm. These magnitudes of p are within the range of values that have been previously used, when p was used as a fitting parameter.[21,22] They also suggest that the model of Lee et al., which treats p as a function of the degree of entanglement of the unrelaxed portion of the long arms at the relaxation time of the shortest arm, rather than as a constant, is a reasonable interpretation of the physical situation.

CDV

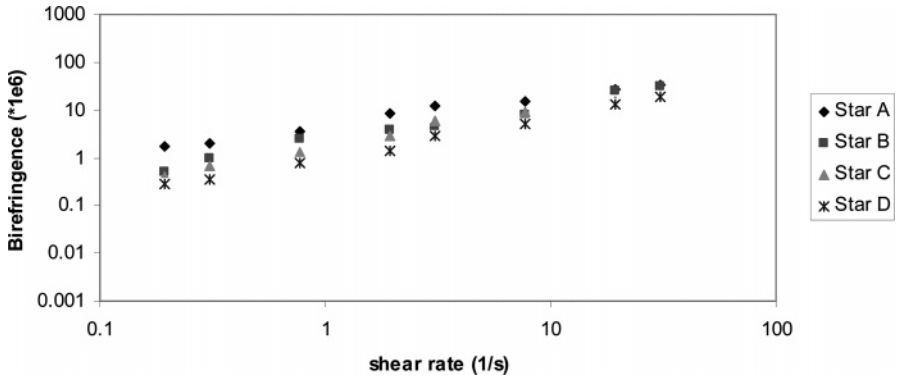

Figure 9. Birefringence plotted as a function of steady-state shear rate for stars A, B, and C and for the linear chain D.

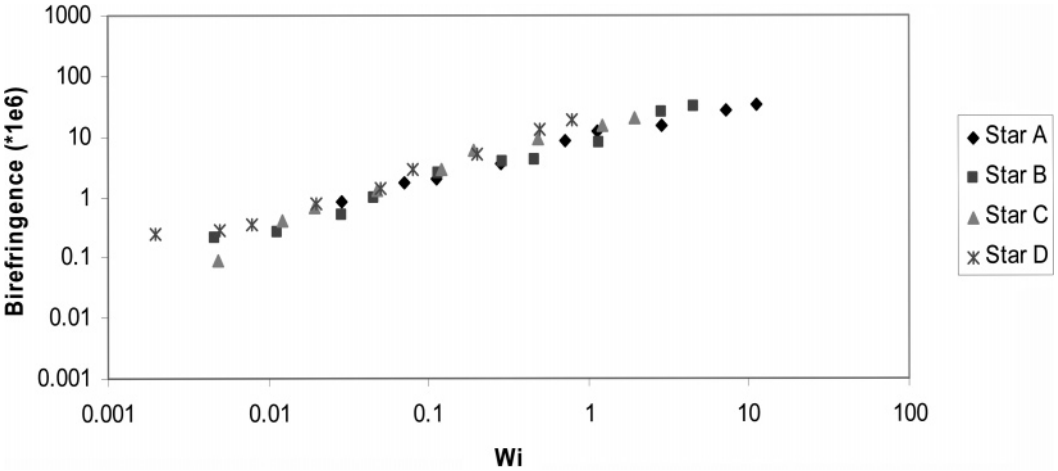

Figure 10. Birefringence plotted as a function of *Wi* for stars A, B, and C and for the linear chain D.

4. Nonlinear Viscoelasticity

We have previously noted that the relaxation behavior of both linear chains and symmetric star polymers in the nonlinear regime is dominated by CCR and further that the exact same model for CCR can be used successfully for both systems. In the remaining sections of this paper, we examine the behavior of asymmetric stars in the nonlinear regime to see whether these same conclusions will also hold for this class of chain architectures.

To probe this question, a series of birefringence measurements were made on the symmetric star A, the two asymmetric stars B and C, and the linear chain D. Specifically, the two-color flow birefringence (TCFB) apparatus was used to determine the steady-state birefringence and orientation angle as a function of shear rate in the same manner as described for symmetric stars by Tezel et al.[4] The stress optical rule was also used to express these results in terms of the shear stress and first normal stress difference. The stress optical rule is generally valid for shear rates less than the inverse Rouse time and thus is applicable to our data, all of which satisfy this condition.

Physically, at shear rates corresponding to a Weissenberg number of $O(1)$, it is expected that there will be a transition from relaxation occurring due to the linear viscoelastic mechanisms of arm length fluctuations, dynamic dilution, and reptation to relaxation dominated by the CCR mechanism. CCR occurs primarily as a consequence of the release of entanglements by the continual retraction of neighboring chains from the stretched configuration that is produced by affine deformation with the flow. This mechanism is a product of chain deformation and retraction rather than the detailed architecture of the polymers. In fact, we have demonstrated in an earlier study that the CCR behavior of linear chains and the arms of symmetric stars is indistinguishable based upon comparisons with experimental rheological and rheooptical data, and so we anticipate that this should also be true for asymmetric stars.

Based on this expectation concerning CCR and our understanding of the linear viscoelastic relaxation mechanisms, some qualitative predictions can be made about how the birefringence and orientation angle should compare for the four solutions that we study here. For a given backbone length, the longest (linear) relaxation time of the star must increase with increasing length of the third (or shorter) arm. This can be understood using the framework of the tube model, as the friction due to the relaxed third arm increasingly suppresses reptation, requiring a larger fraction of the long arms of the star to relax by arm length fluctuations, rather than reptation.

Hence, for a given shear rate, both the birefringence and the departure of the orientation angle from 45° will increase with increasing length of the third arm, as the relaxation by reptation is suppressed. CCR serves to enhance the relaxation of the polymer by removing entanglements with equal probability all along the length of the arm. The impact of this enhanced relaxation is that the birefringence will grow more slowly with shear rate, and the orientation angle will decrease more slowly with shear rate, than if CCR were not present. Later, we will quantify this statement via comparisons with model calculations, both with and without CCR included.

Figure 9 shows the birefringence of each of the four solutions studied here as a function of shear rate. As expected, the trend is that, for a given shear rate, the birefringence does in fact increase with increasing length of the third arm (i.e., with increase in the longest LV relaxation time). At the higher shear

CDV

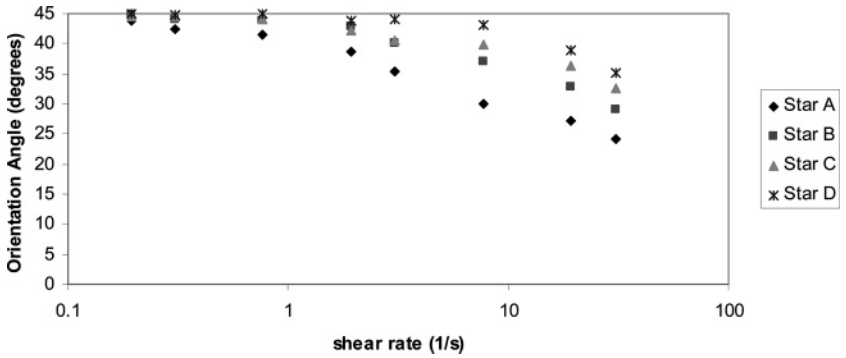

Figure 11. Orientation angle plotted as a function of steady-state shear rate for stars A, B, and C and for the two-armed star, linear chain D.

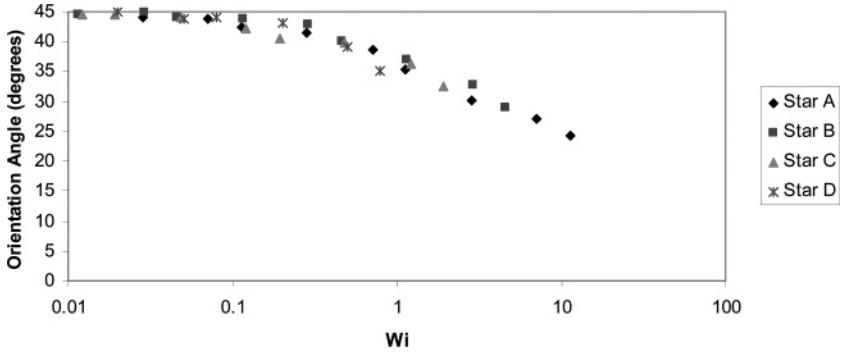

Figure 12. Orientation angle plotted as a function of *Wi* for stars A, B, and C and for the linear chain D.

rates, however, the difference between the measured birefringence is lessened. At the moment it is premature to speculate on the reason for this change. Later, however, we will compare these data with predictions from a model that includes both the linear and CCR contributions to relaxation, and then it will be possible to provide a little additional input.

Figure 10 shows the same experimental results, now plotted as a function of the Weissenberg number, *Wi*, where *Wi* is defined as the shear rate multiplied by the longest relaxation time (Table 2) for each of the four polymer solutions. The longest relaxation times (shown in Figure 6) of the symmetric star A, the two asymmetric stars B and C, and the linear chain D are 0.37, 0.15, 0.063, and 0.026 s, respectively. A value of $Wi = 1$ means that the time scale of the flow is the same as the longest time scale of relaxation of the polymer. The birefringence data in Figure 10 almost collapse onto a single curve. At the lower shear rates, this is presumably because the chain configuration depends on a balance between the deformation due to flow and the LV relaxation process, and the differences in the details of these relaxation mechanisms are less important than the fact that their rates scale with the longest LV relaxation time for each of the four polymers. At the higher shear rates, it is expected that CCR begins to play a role in the chain relaxation, and one might anticipate that the correlation with *Wi* would begin to break down. The relative importance of the LV and CCR relaxation processes will become more evident when we compare these data with model predictions in the next section.

Figure 11 shows the orientation angle as a function of shear rate for the four solutions, and again the trend is as hypothesized, with the orientation angle decreasing with increasing MW of the short arm. The orientation angle represents the competition between alignment by the flow and the relaxation mechanisms. The effectiveness of CCR to relax entanglements increases with increasing shear rate, which means that the rate of reduction of the orientation angle is slowed compared to what would be seen if CCR were not present. In the series of star and linear polymers studied here, at high enough shear rates, it would be expected that the slower relaxation dynamics that led to differences seen in the linear viscoelastic behavior will no longer be manifested, and the behavior of each should begin to converge, as there is a balance between the deformation of the flow and relaxation by CCR. However, in the range of shear rates studied here, there are still significant contributions to the relaxation process due to arm length fluctuations and reptation. Figure 12 shows the orientation angle plotted as a function of *Wi*. Again, the results almost collapse onto a single curve, at least within the precision of the data.

5. Comparisons with a Nonlinear Model

To understand the experimental results from a more quantitative point of view, the next step is to model the behavior of asymmetric stars in shear flow, for the shear rates studied. Clearly, a successful model will have to account for the range of relaxation times along each arm and the transition from relaxation by CLF to relaxation by reptation (where the friction at the branch point depends on the length of the shortest arm), and must also incorporate CCR, to account for the flow induced removal of entanglements. In the present work, we adapt the simple idea for modeling symmetric stars, developed by Tezel et al.,[4] to the case of asymmetric stars. This assumes that the polymer relaxes via the linear viscoelastic modes for times less than the inverse shear rate (which is a measure of the effective relaxation time due to CCR), and the remaining unrelaxed parts of the star arms then relax via CCR. The CCR relaxation process is modeled in what follows below as identical to the model that was previously shown to work for both a linear chain polymer and for the arms of a symmetric 4-arm star.

In the present case, we must distinguish between the short and the long arms of an asymmetric chain. Further, for the linear viscoelastic relaxation process, we adopt the model of Lee et al.[16] Curvilinear coordinates along the short and long arms, s_s and s_l, are defined as the fractional distance from the free end. Based on the equations presented by Lee et al.,[16] a function

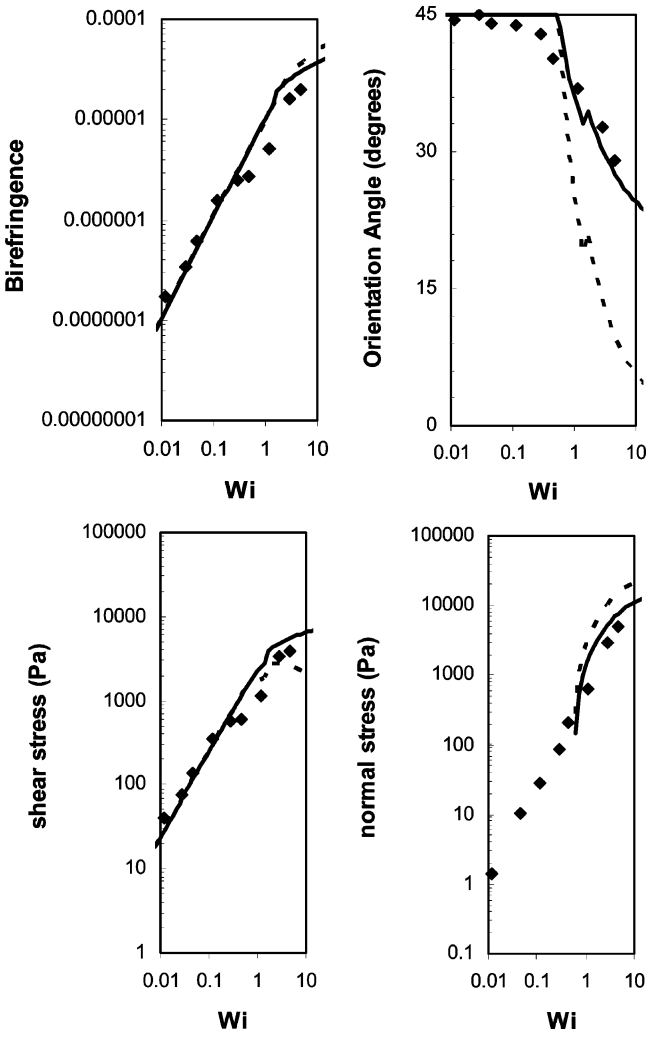

Figure 13. Experimental results and model predictions plotted versus *Wi* for star B. Birefringence, orientation angle, shear stress, and first normal stress difference are shown. Experimental data are shown with discrete points, while model predictions with CCR are shown with a solid line and model predictions without CCR are shown using a dashed line.

$\tau_s(s_s)$ is defined to describe the linear viscoelastic relaxation time at each point along the short arm, as the short arm relaxes by CLF and dynamic dilution. The function $\tau_l(s_l)$ is defined to describe the relaxation time at each point along the long arms, which relax first by CLF and dynamic dilution and then, after the short arm is completely relaxed, by reptation. The next step is to define s_s^* and s_l^* as the points on each arm where the shear rate multiplied by the longest relaxation time at those points is equal to unity. Then each arm is divided into two parts: the end segments ($0 \le s_x < s_x^*$) that possess relaxation rates faster than the inverse shear rates and the interior segments ($s_x^* \le s_x \le 1$) whose relaxation rates are slower. The subscript, x, refers to either "s" for the short arm or "l" for the long arm.

The next step is to define the fraction of the polymer that is short arm, ϕ_s, and the fraction that is long arm, ϕ_l:

$$\phi_s = \frac{Z_s}{Z_s + 2Z_l} \tag{4}$$

$$\phi_l = 1 - \phi_s \tag{5}$$

Z_s and Z_l are the number of entanglements in the short and long arms, respectively.

With these definitions, equations can be written for the steady-state shear stress and first normal stress difference as functions of the shear rate. Without CCR the shear stress is standard linear response theory transformed to steady shear flow that includes contributions from the short arms and long arms:

$$\sigma_{12} = \phi_s\dot{\gamma}G_N^0\int_0^{s_s^*(\dot{\gamma})}\tau_s(s_s)(1-s_s)\,ds_s + \phi_l\dot{\gamma}G_N^0\int_0^{s_l^*(\dot{\gamma})}\tau_l(s_l)(1-s_l)\,ds_l \tag{6}$$

The equation for the shear stress that includes CCR has two additional terms, which account for CCR acting on the interior segments of the arms that have a relaxation time that is longer than the time scale of the flow. The prefactor for these terms is taken directly from the application of CCR to linear polymers and symmetric star polymers:[4,26]

$$\sigma_{12} = \phi_s\dot{\gamma}G_N^0\int_0^{s_s^*(\dot{\gamma})}\tau_s(s_s)(1-s_s)\,ds_s + \phi_l\dot{\gamma}G_N^0\int_0^{s_l^*(\dot{\gamma})}\tau_l(s_l)(1-s_l)\,ds_l + 0.6\phi_sG_N^0(1-s_s^*(\dot{\gamma}))^2 + 0.6G_N^0\phi_l(1-s_l^*(\dot{\gamma}))^2 \tag{7}$$

Similarly, equations can be proposed to predict the first normal stress difference as a function of shear rate with (eq 8) and without CCR (eq 9). There is no linear viscoelastic contribution from the outer part of the arms. In the absence of CCR, the interior regions of the arms are fully aligned in the flow direction, and this produces a first normal stress contribution, which after accounting for dynamic dilution and the relevant fraction of the chain, is

$$N_1 = 3.0\phi_sG_N^0(1-s_s^*(\dot{\gamma}))^2 + 3.0\phi_lG_N^0(1-s_l^*(\dot{\gamma}))^2 \tag{8}$$

The inclusion of CCR means that the interior portions of the arms are not completely aligned, and thus the magnitude of the normal stress contribution is reduced. If the prefactor that was found to work best for linear polymers and symmetric stars is applied to the asymmetric star arms, the first normal stress difference becomes

$$N_1 = 1.55\phi_sG_N^0(1-s_s^*(\dot{\gamma}))^2 + 1.55\phi_lG_N^0(1-s_l^*(\dot{\gamma}))^2 \tag{9}$$

As expected, the first normal stress difference is always positive. This simply implies that a positive tensile stress must be applied in the flow direction to maintain the system in the aligned (nonequilibrium) state.

Model predictions are made for stars B and C, using the parameters that led to the best fit of the LVE data. This means that there are no adjustable parameters. A comparison of the model predictions and the experimental results for stars B and C is shown in Figures 13 and 14, respectively. In both cases, the model that includes CCR leads to a better fit with the experimental data.

CCR enhances relaxation beyond what would be expected without CCR, leading to additional orientation relaxation. In the case of the orientation angle, the differences between predictions that include and exclude CCR are the most dramatic. Without CCR, the unrelaxed portions of the arm are assumed to be completely aligned with the flow, leading to an orientation angle that quickly drops once shear rates are larger than the inverse of the longest relaxation time. CCR relaxes the interior segments of the star, leading to a larger orientation angle for a given shear rate, and one that agrees much better with the experimental data. This indicates that CCR occurs in asymmetric

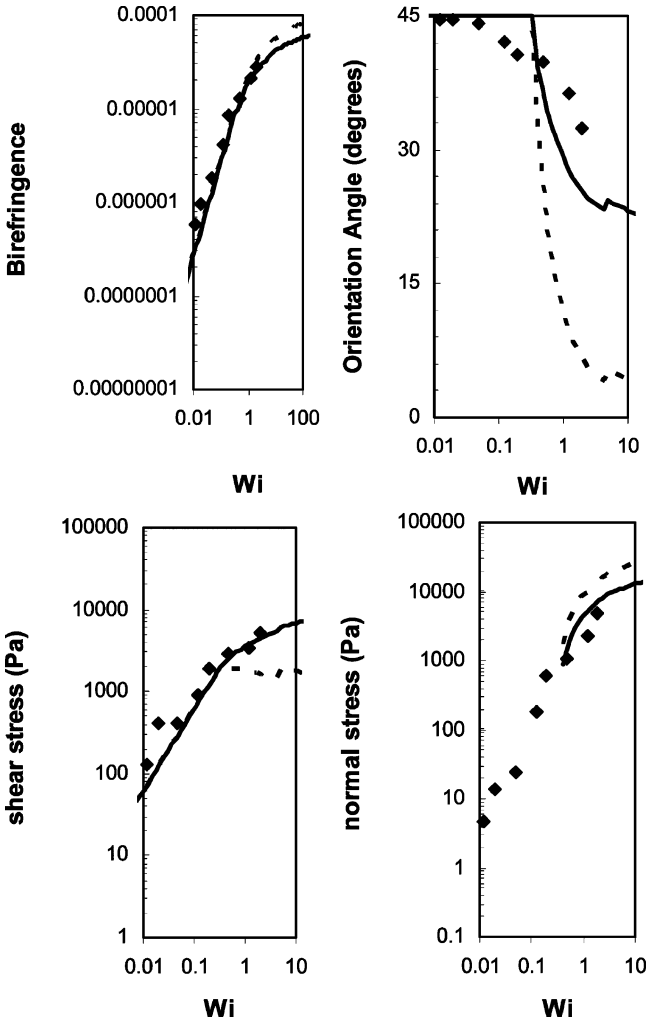

Figure 14. Experimental results and model predictions plotted versus *Wi* for star C. Birefringence, orientation angle, shear stress, and first normal stress difference are shown. Experimental data are shown with discrete points, while model predictions with CCR are shown with a solid line and model predictions without CCR are shown using a dashed line.

stars and can be accounted for in the same way as it has been accounted for in symmetric stars. The model predictions for the shear stress show that a shear stress maximum is predicted when CCR is not present. As has been demonstrated for linear chains and stars, the addition of CCR leads to elimination of the physically unrealizable shear stress maximum.[4,27]

In comparing the fit of the data and the predictions for the two stars, it can be observed that star C shows a larger deviation from orientation angle predictions once the orientation angle drops below 45° than star B. The reason that the models predict a sharp drop-off from 45° rather than a smooth decrease in orientation angle as seen experimentally is that there is an assumption built into the model. This assumption is that the linear viscoelastic relaxation times for points on an arm with curvilinear coordinate s_l larger than s_l^* are much longer than the relaxation times due to CCR. This is a good approximation provided the LV relaxation mechanism for those points is CLF because these relaxation times increase exponentially with s_1. The assumption breaks down, however, as the chain becomes more "linear-like", and reptation relaxes a larger fraction of the star. Hence, it breaks down as the difference between the relaxation times of the short and long arms increases. Because star C has a larger fraction that relaxes by reptation than star B, it shows a larger deviation from the model predictions. This same assumption also leads to model predictions of a first normal stress difference that is completely absent until $Wi = 1$. This is again based on the idea that all segments are completely relaxed by reptation and CLF before they are affected by the flow and thus are unable to contribute to any first normal stress difference. The measurements of a nonzero first normal stress difference for $Wi < 1$ are due to the breakdown of the assumption of a large separation between time scales.

6. Conclusions

We have successfully synthesized a series of asymmetric, polybutadiene stars having the same backbone arms in significant quantities, and we have examined the rheological behavior of entangled solutions of these polymers in both the linear and nonlinear viscoelastic regimes.

In the linear viscoelastic regime, we compared our data with the recent model of Lee et al. In accord with previously presented model/data comparisons, our results demonstrate that the model provides a reasonable qualitative description of the observed behavior but differs quantitatively when we allow only the relaxation time scale τ_e as a fitting parameter, rather than using two or more of the quantities M_e, G_N^0, and τ_e as adjustable parameters as previous investigators have done. The predicted p values are within the range of those previously used and are found to increase with increasing length of the short arm, in qualitative accord with the recent model of Lee et al.

In the nonlinear regime, the first experimental results for the response of entangled asymmetric stars to steady shear have been presented and are compared to a simple theoretical model based upon the ideas developed recently for symmetric stars, together with the linear viscoelastic model of Lee et al. The qualitative agreement between the experimental results and the model predictions when CCR is included again indicates that CCR is an important relaxation mechanism once shear rates reach the inverse of the longest relaxation time and, further, that a simple model of CCR for linear chains can be applied directly to describe the relaxation of chain orientation on the arms of either symmetric or asymmetric stars.

References and Notes

(1) Adams, C. H.; Brereton, M. B.; Hutchings, L. R.; Klein, P. G.; McLeish, T. C. B.; Richards, R. W.; Ries, M. E. *Macromolecules* **2000**, *33*, 7101−7106.
(2) Adams, C. H.; Hutchings, L. R.; Klein, P. G.; McLeish, T. C. B.; Richards, R. W. *Macromolecules* **1996**, *29*, 5717−5722.
(3) Ye, X.; Sridhar, T. *Macromolecules* **2001**, *34*, 8270−8277.
(4) Tezel, A. K.; Leal, L. G.; McLeish, T. C. B. *Macromolecules* **2005**, *38*, 1451−1455.
(5) Osaki, K.; Takatori, E.; Kurata, M.; Watanabe, H.; Yoshida, H.; Kotaka, T. *Macromolecules* **1990**, *23*, 4392−4396.
(6) Fetters, L. J.; Kiss, A. D.; Pearson, D. S.; Quack, G. F.; Vitus, F. J. *Macromolecules* **1993**, *26*, 647−654.
(7) Santangelo, P. G.; Roland, C. M.; Puskas, J. E. *Macromolecules* **1999**, *32*, 1972−1977.
(8) Pearson, D. S.; Helfand, E. *Macromolecules* **1984**, *17*, 888−895.
(9) Watanabe, H.; Matsumiya, Y.; Inoue, T. *Macromolecules* **2002**, *35*, 2339−2357.
(10) Watanabe, H.; Matsumiya, Y.; Osaki, K. *J. Polym. Sci., Part B: Polym. Phys.* **2000**, *38*, 1024−1036.
(11) Milner, S. T.; McLeish, T. C. B. *Macromolecules* **1997**, *30*, 2159−2166.
(12) Milner, S. T.; McLeish, T. C. B. *Macromolecules* **1998**, *31*, 7479−7482.
(13) McLeish, T. C. B. *Adv. Phys.* **2002**, *51*, 1379−1527.
(14) McLeish, T. C. B.; Milner, S. T. *Adv. Polym. Sci.* **1999**, *143*, 195−256.
(15) Milner, S. T.; McLeish, T. C. B. *Phys. Rev. Lett.* **1998**, *81*, 725−728.
(16) Lee, J. H.; Fetters, L. J.; Archer, L. A. *Macromolecules* **2005**, *38*, 4484−4494.
(17) Likhtman, A. E.; Milner, S. T.; McLeish, T. C. B. *Phys. Rev. Lett.* **2000**, *85*, 4550−4553.

(18) Tezel, A. K. Nonlinear Rheology of Entangled Symmetric and Asymmetric Star Polymers. Dissertation. In: *Chemical Engineering*; University of California, Santa Barbara, 2005.
(19) Gell, C. B.; Graessley, W. W.; Efstratiadis, V.; Pitsikalis, M.; Hadjichristidis, N. *J. Polym. Sci., Part B: Polym. Phys.* **1997**, *35*, 1943−1954.
(20) Pennisi, R. W.; Fetters, L. J. *Macromolecules* **1988**, *21*, 1094−1099.
(21) Park, S. J.; Shanbhag, S.; Larson, R. G. *Rheol. Acta* **2005**, *44*, 319−330.
(22) Blackwell, R. J.; McLeish, T. C. B.; Harlen, O. G. *J. Rheol.* **2000**, *44*, 121−136.
(23) Archer, L. A.; Juliani. *Macromolecules* **2004**, *37*, 1076−1088.
(24) Daniels, D. R.; McLeish, T. C. B.; Crosby, B. J.; Young, R. N.; Fernyhough, C. M. *Macromolecules* **2001**, *34*, 7025−7033.
(25) Frischknecht, A. L.; Milner, S. T.; Pryke, A.; Young, R. N.; Hawkins, R.; McLeish, T. C. B. *Macromolecules* **2002**, *35*, 4801−4820.
(26) Milner, S. T.; McLeish, T. C. B.; Likhtman, A. E. *J. Rheol.* **2001**, *45*, 539−563.
(27) Marrucci, G. *J. Non-Newtonian Fluid Mech.* **1996**, *62*, 279−289.

MA0601520